Published in final edited form as:

Sci Transl Med. 2017 March 15; 9(381): . doi:10.1126/scitranslmed.aai7514.

Staged induction of HIV-1 glycan–dependent broadly neutralizing antibodies

Mattia Bonsignori[1,2,*,†], **Edward F. Kreider**[3,†], **Daniela Fera**[4,†], **R. Ryan Meyerhoff**[1,2,†], **Todd Bradley**[1,2,†], **Kevin Wiehe**[1,2], **S. Munir Alam**[1,2], **Baptiste Aussedat**[5], **William E. Walkowicz**[5], **Kwan-Ki Hwang**[2], **Kevin O. Saunders**[2,6], **Ruijun Zhang**[2], **Morgan A. Gladden**[2], **Anthony Monroe**[2], **Amit Kumar**[2], **Shi-Mao Xia**[2], **Melissa Cooper**[2], **Mark K. Louder**[7], **Krisha McKee**[7], **Robert T. Bailer**[7], **Brendan W. Pier**[4], **Claudia A. Jette**[4], **Garnett Kelsoe**[2,8], **Wilton B. Williams**[1,2], **Lynn Morris**[9], **John Kappes**[10], **Kshitij Wagh**[11], **Gift Kamanga**[12,‡], **Myron S. Cohen**[13], **Peter T. Hraber**[11], **David C. Montefiori**[2,6], **Ashley Trama**[2], **Hua-Xin Liao**[1,2], **Thomas B. Kepler**[14], **M. Anthony Moody**[2,8,15], **Feng Gao**[1,2], **Samuel J. Danishefsky**[5], **John R. Mascola**[7], **George M. Shaw**[3], **Beatrice H. Hahn**[3], **Stephen C. Harrison**[4], **Bette T. Korber**[11,*,†], and **Barton F. Haynes**[1,2,*,†]

[1]Department of Medicine, Duke University School of Medicine, Duke University Medical Center, Durham, NC 27710, USA

[2]Duke Human Vaccine Institute, Durham, NC 27710, USA

[3]Departments of Medicine and Microbiology, Perelman School of Medicine, University of Pennsylvania, Philadelphia, PA 19104, USA

[*]Corresponding author. mattia.bonsignori@dm.duke.edu (M.B.); btk@lanl.gov (B.T.K.); barton.haynes@dm.duke.edu (B.F.H.).
[†]These authors contributed equally to this work.
[‡]Present address: FHI 360, Lilongwe, Malawi.

SUPPLEMENTARY MATERIALS

www.sciencetranslationalmedicine.org/cgi/content/full/9/381/eaai7514/DC1

Materials and Methods

References (*36*–*52*)

Author contributions: M.B., B.H.H., S.C.H., B.T.K., and B.F.H. coordinated and designed the study, analyzed and evaluated the data, and wrote and edited the manuscript and figures; E.F.K., D.F., T.B., K. Wiehe, K.O.S., A.M., and S.M.A. performed experiments, analyzed the data, and produced the figures; M.B. directed the memory B cell cultures and performed intrinsic mutability analysis; R.R.M. isolated the antibodies through antigen-specific single-cell sorting; D.F., B.W.P., and C.A.J. performed structural studies; B.A., W.E.W., and S.J.D. synthesized the Man9-V3 glycopeptide; K.-K.H., M.A.G., and A.M. executed the memory B cell cultures and antibody functional screenings; R.Z., A.T., H.-X.L., A.K., and F.G. produced the recombinant proteins and pseudoviruses; S.-M.X., M.C., M.K.L., K.M., R.T.B., J.R.M., and D.C.M. performed neutralization studies; G. Kelsoe, J.R.M., and G.M.S. provided intellectual contributions; W.B.W., L.M., and J.K. contributed the NGS data, CH848 plasma profiling, and transfected cell lines, respectively; K. Wagh, P.T.H., and B.T.K. performed virus signature and virus evolution analyses; G. Kamanga and M.S.C. supervised the clinical sites; M.A.M. supported single-cell sorting; T.B.K. performed computational analysis; and B.F.H. conceived the study. All authors approved the paper.

Competing interests: M.B., R.R.M., M.A.M., H.-X.L., T.B., K.O.S., P.T.H., B.T.K., and B.F.H. have filed patent application(s) covering DH270 lineage antibodies and immunogens to induce such antibodies. B.A., H.-X.L., B.F.H., and S.J.D. have filed patent application(s) covering the V3 glycopeptide and its synthesis and use as an immunogen. All other authors declare that they have no competing interests.

Data and materials availability: The V(D)J rearrangement sequences of DH272, DH475, and the DH270 lineage antibodies (DH270.UCA, DH270.IA1 to DH270.IA4, and DH270.1 to DH270.6) have been deposited in GenBank, with accession numbers KY354938 to KY354963. NGS sequence data for clones DH270, DH272, and DH475 have been deposited in GenBank, with accession numbers KY347498 to KY347701. Coordinates and structure factors for UCA1, UCA3, DH270.1, DH270.3, DH270.5, DH270.6, and DH272 have been deposited in the PDB, with accession code 5U0R, 5U15, 5U0U, 5TPL, 5TPP, 5TQA, and 5TRP, respectively. The EM map of the 92BR SOSIP.664 trimer in complex with DH270.1 has been deposited in the EM Data Bank, with accession code EMD-8507.

[4]Laboratory of Molecular Medicine, Boston Children's Hospital, Harvard Medical School, Boston, MA 02115, USA

[5]Department of Chemical Biology, Memorial Sloan Kettering Cancer Center, New York, NY 10065, USA

[6]Department of Surgery, Duke University School of Medicine, Duke University Medical Center, Durham, NC 27710, USA

[7]Vaccine Research Center, National Institute of Allergy and Infectious Diseases, National Institutes of Health, Bethesda, MD 20892, USA

[8]Department of Immunology, Duke University School of Medicine, Duke University Medical Center, Durham, NC 27710, USA

[9]National Institute for Communicable Diseases, Johannesburg 2131, South Africa

[10]Department of Medicine, University of Alabama at Birmingham, Birmingham, AL 35294, USA

[11]Los Alamos National Laboratory, Los Alamos, NM87545, USA

[12]University of North Carolina Project, Kamuzu Central Hospital, Lilongwe, Malawi

[13]Departments of Medicine, Epidemiology, and Microbiology and Immunology, University of North Carolina, Chapel Hill, NC 27599, USA

[14]Department of Microbiology and Department of Mathematics and Statistics, Boston University, Boston, MA 02215, USA

[15]Department of Pediatrics, Duke University School of Medicine, Duke University Medical Center, Durham, NC 27710, USA

Abstract

A preventive HIV-1 vaccine should induce HIV-1–specific broadly neutralizing antibodies (bnAbs). However, bnAbs generally require high levels of somatic hypermutation (SHM) to acquire breadth, and current vaccine strategies have not been successful in inducing bnAbs. Because bnAbs directed against a glycosylated site adjacent to the third variable loop (V3) of the HIV-1 envelope protein require limited SHM, the V3-glycan epitope is an attractive vaccine target. By studying the cooperation among multiple V3-glycan B cell lineages and their coevolution with autologous virus throughout 5 years of infection, we identify key events in the ontogeny of a V3-glycan bnAb. Two autologous neutralizing antibody lineages selected for virus escape mutations and consequently allowed initiation and affinity maturation of a V3-glycan bnAb lineage. The nucleotide substitution required to initiate the bnAb lineage occurred at a low-probability site for activation-induced cytidine deaminase activity. Cooperation of B cell lineages and an improbable mutation critical for bnAb activity defined the necessary events leading to breadth in this V3-glycan bnAb lineage. These findings may, in part, explain why initiation of V3-glycan bnAbs is rare, and suggest an immunization strategy for inducing similar V3-glycan bnAbs.

INTRODUCTION

A vaccine to prevent HIV-1 infection should include immunogens that can induce broadly neutralizing antibodies (bnAbs) (1, 2). Of the five major targets for bnAbs, the glycan-rich apex of the HIV-1 envelope (Env) trimer and the base of the third variable loop (V3) are distinguished by the potency of antibodies directed against them (3–8). Although these antibodies have less breadth than those directed against the CD4-binding site (CD4bs) or the gp41 membrane-proximal external region (MPER), one current goal of vaccine development is to elicit them in combination with other bnAb specificities to achieve broad coverage of transmitted/founder (TF) viruses to prevent HIV-1 integration upon exposure (1, 2).

Mapping the coevolution of virus and antibody lineages over time informs vaccine design by defining the succession of HIV-1 Env variants that evolve in vivo during the course of bnAb development (9–11). Antibody lineages with overlapping specificities can influence each other's affinity maturation by selecting for synergistic or antagonistic escape mutations: an example of such "cooperating" lineages is provided by two CD4bs-directed bnAbs that we characterized previously (11, 12). Thus, cooperating antibody lineages and their viral escape mutants allow identification of the specific Envs, among the diverse repertoire of mutated Envs that develop within the autologous quasi-species in the infected individual, that stimulate bnAb development and that we wish to mimic in a vaccine.

Here, we describe the coevolution of an HIV-1 Env quasi-species and a memory B cell lineage of gp120 V3-glycan–directed bnAbs in an acutely infected individual followed over time as broadly neutralizing plasma activity developed. To follow virus evolution, we sequenced ~1200 HIV-1 *env* genes sampled over a 5-year period; to follow the antibody response, we identified natural heavy- and light-chain pairs of six antibodies from a bnAb lineage, designated DH270, and augmented this lineage by next-generation sequencing (NGS). Structural studies defined the position of the DH270 Fab on gp140 Env. We also found two B cell lineages (DH272 and DH475) with neutralization patterns that likely selected for observed viral escape variants, which, in turn, stimulated the DH270 lineage to potent neutralization breadth. We found a mutation in the DH270 heavy chain that occurred early in affinity maturation at a disfavored activation-induced cytidine deaminase (AID) site and that was necessary for bnAb lineage initiation. This improbable mutation can explain the long period of antigenic stimulation needed for initial expansion of the bnAb B cell lineage in this individual.

RESULTS

Three N332 V3-glycan–dependent antibody lineages

We studied an African male from Malawi (CH848) followed from the time of infection up to 5 years after transmission. He was infected with a clade C virus, developed plasma neutralization breadth 3.5 years after transmission, and did not receive antiretroviral therapy during this time as per country treatment guidelines. Reduced plasma neutralization of N332A Env–mutated HIV-1 pseudoviruses and plasma neutralization fingerprinting demonstrated the presence of N332-sensitive bnAbs (table S1) (13). To identify these antibodies, we studied memory B cells from weeks 205, 232, and 234 after infection using

memory B cell cultures (14) and antigen-specific sorting (15, 16) and found three N332-sensitive lineages, designated DH270, DH272, and DH475. Their genealogy was augmented by the NGS of memory B cell complementary DNA from seven time points from week 11 to week 240 after transmission.

DH270 antibodies were recovered from memory B cells at all three sampling times (weeks 205, 232, and 234), and expansion of the clone did not occur until week 186 (Fig. 1A and table S2). Clonal expansion was concurrent with the development of plasma neutralization breadth (tableS3), and members oftheDH270 lineage also displayed neutralization breadth (Fig. 1B and data set S1). The most potent DH270 lineage bnAb (DH270.6) was isolated using a fluorophore-labeled Man_9-V3 glycopeptidethatisamimicoftheV3-glycan bnAb epitope (16), which comprises a discontinuous 30–amino acid residue peptide segment within gp120 V3 and is representative of the PGT128-bound minimal epitope described by Pejchal *et al.* (17). The synthetic Man_9-V3 glycopeptide includes high-mannose glycan residues (Man_9) each at N301 and N332 and was synthesized using a chemical process similar to that described previously (18, 19). The V3-glycan bnAb PGT128 affinity for the Man_9-V3 glycopeptide was similar to that of PGT128 for the BG505 SOSIP trimer, and Man_9-V3 glycopeptide was therefore an effective affinity bait for the isolation of V3-glycan bnAbs (16). The lineage derived from a *V_H1–2*02* rearrangement that produced a CDRH3 [complementarity-determiningregion(CDR)H3]of20–amino acid residues paired with a light chain encoded by *$V_\lambda 2$–23* (fig. S1). Neutralization assays and competition with theV3-glycan bnAbs PGT125 and PGT128 confirmed dependence of lineage on the potential N-linked glycosylation (PNG) site at N332 (fig. S2).

The DH475 mAb was recovered from memory B cells at week 232 after transmission by antigen-specific sorting using the fluorophore-labeled Man_9-V3 glycopeptide (16). The earliest DH475 lineage $V_H(D)J_H$ rearrangements were identified with the use of NGS at week 64 after transmission (fig. S3A and table S2). Its heavy chain came from *V_H3–23*01* [V_H (variable gene of immunoglobulin heavy chain) mutation frequency, 10.1%] paired with a *$V_\lambda 4$–69*02* light chain (fig. S3B).

The DH272 mAb came from cultured memory B cells obtained at week 205 after transmission. DH272 lineage $V_H(D)J_H$ rearrangements were detected as early as 19 weeks after transmission by NGS (fig. S3A and table S2). The DH272 heavy chain used *V_H1–2*02*, as did DH270, but it paired with a *$V_\kappa 2$–30* light chain. Its CDR H3 was 17 amino acids long; V_H mutation was 14.9%. DH272, an immunoglobulin A (IgA) isotype, had a six-nucleotide deletion in FR H3 (fig. S3B).

For both DH272 and DH475 lineages, binding to CH848 TF Env gp120 depended on the N332 PNG site (fig. S3C). DH272 binding also depended on the N301 PNG site (fig. S3C). Neither lineage had neutralization breadth (fig. S3D).

Evolution of the CH848 virus quasi-species

We sequenced 1223 HIV-1 3′ half single genomes from the virus in plasma collected at 26 time points over 246 weeks. Analysis of sequences from the earliest plasma sample indicated that CH848 had been infected with a single, subtype clade C founder virus, ~ 17

(confidence interval, 14 to 19) days before screening (figs. S4 and S5). By week 51 after infection, 91% of the sequences had acquired an identical 10-residue deletion in variable loop 1 (V1), a region that includes the PGT128-proximal residues 133 to 135 and 141 (figs. S6 and S7). Further changes accrued during the ensuing 4 years, including additional insertions and deletions in V1, mutations in the ^{324}GDIR^{327} motif within the V3 loop, deletion or shifting of N-linked glycosylation sites at positions 301 and 322, and mutations at PGT128-proximal positions in V1, V3, and C4; however, none of these escape variants went to fixation during the 4.5 years of follow-up (figs. S6 to S9).

Simultaneous with the first detection of DH270 lineage antibodies at week 186, four autologous virus clades emerged, which defined distinct immunological resistance profiles of the CH848 autologous quasi-species (fig. S6). The first clade included viruses that shifted the PNG site at N332 to N334 (fig. S6, open circles), and despite the fact that this mutation was associated with complete resistance to the DH270 lineage bnAbs, this clade was detected only transiently and at a relatively low frequency (7 to 33% per sample), suggesting a balance where immune escape was countered by a cost in virological fitness. Conversely, viruses in the other three clades retained N332 and persisted throughout the 5 years of sampling. Viruses in the second clade resisted DH270 lineage neutralization and comprised gp120 Envs that were not bound by the DH270 antibodies (fig. S6, triangles, and data set S2). The third and fourth clades defined autologous viruses whose gp120 Env was bound by DH270 lineage antibodies but that were either only weakly neutralized by the most mature members of the DH270 lineage (fig. S6, “X,” and data set S2) or completely neutralization-resistant (fig. S6, “+,” and data set S2), respectively. Persistence of four divergent clades in the CH848 Env, each with distinctive immunological resistance phenotypes, suggests that multiple distinctive immune escape routes were explored and selected, allowing continuing Env escape mutations to accrue in distinct frameworks and exposing the antibody to Env diversity that may have been necessary to acquire neutralization breadth.

Ontogeny of DH270 lineage and acquisition of neutralization breadth

As with other V3-glycan bnAbs, viral neutralization clade specificity and intraclade breadth of DH270 depended primarily on the frequency of the N332 glycosylation site within the relevant clade (Fig. 2A). Only 1 of the 62 pseudoviruses tested that lacked the PNG site at N332, the B clade virus 5768.04, was sensitive to DH270.5 and DH270.6 (data set S1). Across the full panel of M group HIV-1 virus isolates used in neutralization assays, the loss of the PNG N332 sites accounted for 70% of the observed neutralization resistance. The circulating recombinant form CRF01 rarely has this glycosylation site [3% of sequences in the Los Alamos database and 4% (1 of 23) in our test panel], and the DH270 lineage antibodies did not neutralize CRF01 strains (Fig. 2A). As a consequence of the N332 PNG site requirement of V3-glycan bnAbs to neutralize, in vitro estimation of neutralizing breadth was affected simply by the fraction of CRF01 viruses included in the panel. Other V3-glycan bnAbs (10-1074, PGT121, and PGT128) shared this N332 glycan dependency, but PGT121 and PGT128 were not as restrictive (data set S1) (5, 6, 8). Antibody 10-1074 was similar to DH270.6, in that it more strictly required the N332 PNG site, and its neutralization potency correlated with that of DH270.6 (Pearson’s $r = 0.63$, $P = 8.0 \times 10^{-13}$) (8).

Heterologous breadth and potency of the DH270 lineage antibodies increased with the accumulation of V_H mutations, and although DH270.UCA did not neutralize heterologous HIV-1, five amino acid substitutions in DH270.IA4 (four in the heavy chain and one in the light chain) were sufficient to initiate the bnAb lineage and confer heterologous neutralization (Fig. 2, B and C, and data set S3).

The capacity of the early DH270 lineage members to neutralize heterologous viruses correlated with the presence of short V1 loops (Fig. 2D). As the lineage evolved, it gained capacity to neutralize viruses with longer V1 loops, although with reduced potency (Fig. 2D and fig. S10, A to C). Neutralization of the same virus panel by the V3-glycan bnAbs 10-1074, PGT121, and PGT128 followed the same inverse correlation between potency and V1 length (fig. S10, D to F).

Mutations in the DH270 antibody lineage that initiated heterologous neutralization

The likelihood of AID-generated somatic mutation in immunoglobulin genes has strong nucleotide sequence dependence (20, 21). Moreover, we have recently shown for CD4bs bnAbs that V_H sites of high intrinsic mutability determine many sites of somatic hypermutation (11). Like the VRC01-class CD4bs bnAbs, both DH270 and DH272 used *V_H1–2*02*, although unlike the CD4bs bnAbs, V3-glycan bnAbs in general can use quite disparate V_H gene segments (3, 17, 22–25). Antibodies in both lineages have mutations at the same amino acid positions that correspond to sites of intrinsic mutability that we identified in the *V_H1–2*02* CD4bs bnAbs (fig. S11A) (11). In HIV-1–negative individuals, we identified 20 amino acids that frequently mutate from the *V_H1–2*02* germline sequence (fig. S11A). Twelve of these 20 amino acids were also frequently mutated in the DH270 lineage antibodies, and 11 of these 12 amino acids mutated to 1 of the 2 most frequent amino acids mutated in non–HIV-1 *V_H1–2*02* sequences (identity conformity). G57R was the lone exception. DH272 mutated in 6 of these 12 positions, and CD4bs bnAb VRC01 mutated in 11 of 12 positions (fig. S11A).

The presence of the canonical *V_H1–2*02* allele in individual CH848 was confirmed by genomic DNA sequencing (fig. S11B). Four nucleotide changes in the DH270.UCA conferred heterologous neutralization activity on the next intermediate antibody (IA4). The G92A and G102A nucleotide mutations in DH270.IA4 (and in DH272) occurred at "canonical" AID hotspots (DGYW) and encoded amino acid substitutions G31D and M34I, respectively (Fig. 3A). G164C (G164A for DH272) was in a "noncanonical" AID hotspot with a comparable level of mutability (20) and encoded the S55T (N for DH272) substitution (Fig. 3A). In contrast, the G169C mutation in DH270.IA4, which encoded the G57R amino acid mutation, occurred at a site with a very low predicted level of mutability (20), generated a canonical cold spot (GTC), and disrupted the overlapping AID hotspot at G170 within the same codon, which was instead used by DH272 and resulted in the G57V substitution (Fig. 3A). Thus, although both the DH270 bnAb and DH272 autologous neutralizing lineages had mutations at Gly^{57}, the substitution in the DH270 lineage (G57R) was an improbable event, whereas the substitution (G57V) in the DH272 lineage was much more probable.

The G31D and M31I substitutions that occurred in AID hotspots became fixed in both lineages, and S55T eventually became prevalent also in the DH272 lineage (Fig. 3B). By week 111 after transmission, all DH272 lineage $V_H(D)J_H$ transcripts sequenced by NGS harbored a mutation in the Gly^{57} codon, which resulted in the predominance of an encoded aspartic acid (Fig. 3B). In contrast, only 6 of 758 (0.8%) DH270 lineage transcripts isolated 186 weeks after transmission had Val^{57} or Asp^{57}; 48 of 758 (6.3%) retained Gly^{57}, whereas over two-thirds, 514 of 758 (67.8%), had G57R (Fig. 3B).

Because the rare G169C nucleotide mutation in DH270.IA4 introduced a cold spot and simultaneously disrupted the overlapping AID hotspot, it had a high probability of being maintained once it occurred, and indeed, it was present in 523 of 758 (68%) DH270 lineage V_H sequences identified with NGS at week 186 after transmission (Fig. 3C).

Reversion of Arg^{57} to Gly abrogated DH270.IA4 neutralization of autologous and heterologous HIV-1 isolates (Fig. 3D). A DH270.IA4 R57V mutant (with the base change that would have occurred had the overlapping AID hotspot been used) also greatly reduced DH270.IA4 neutralization, confirming that Arg^{57}, rather than the absence of Gly^{57}, was responsible for the acquired neutralizing activity (Fig. 3D). Finally, the DH270. UCA G57R mutant neutralized both autologous and heterologous viruses, confirming that G57R alone could confer neutralizing activity on the DH270 germline antibody (Fig. 3E). Thus, the improbable G169C mutation conferred reactivity against autologous virus and initiated acquisition of heterologous neutralization breadth in the DH270 lineage.

A search for an Env that might select for the critical G57R mutation in DH270. UCA or IA4-like antibodies yielded Env 10.17 at week 135 of infection (fig. S12, A and B), which derived from the only autologous virus Env that DH270.IA4 could bind. DH270.IA4 binding to Env 10.17 depended on the presence of Arg^{57}, and reversion of Arg^{57} to Gly (R57G) was necessary and sufficient to abrogate binding (fig. S12A). Also, binding to Env 10.17 was acquired by DH270.UCA upon introduction of the G57R mutation (fig. S12B).

Autologous neutralizing antibody lineages that cooperated with DH270

Evidence for functional interaction among the three N332-dependent lineages came from the respective neutralization profiles against a panel of 90 autologous viruses from TF to week 240 after transmission (Fig. 4A and data set S2). Both DH475 and DH272 neutralized autologous viruses isolated during the first year of infection, which were resistant to most DH270 lineage antibodies (only DH270. IA1 and DH270.4 neutralized weakly) (Fig. 4A). DH475 neutralized viruses from week 15 to week 39, and DH272 neutralized the CH848 TF and all viruses isolated up to week 51, when viruses that resisted DH475 and DH272 became strongly sensitive to the more mature antibodies in the DH270 lineage (V_H nucleotide mutation frequency, ≥5.6%) (Fig. 4A).

The identification of specific mutations implicated in the switch of virus sensitivity was complicated by the high levels of mutations accumulated by virus Env over time (fig. S13 and data set S4). We identified virus signatures that defined the DH270.1 and DH272/DH475 immunotypes and introduced four of them, in various combinations, into the DH272/DH475-sensitive virus that was closest in sequence to the DH270.1-sensitive immunotype: a

10–amino acid deletion in V1 (Δ134–143); a D185N mutation in V2, which introduced an N-linked glycosylation site; an N413Y mutation in V4, which disrupted an N-linked glycosylation site; and a 2–amino acid deletion (Δ463–464) in V5.

The large V1 deletion was critical for DH270.1 neutralization, with smaller contributions from the other changes; the V1 deletion increased virus resistance to DH475 (3.5-fold increase). V1 loop– mediated resistance to DH475 neutralization increased further when combined with the Δ463–464 V5 deletion (5-fold increase) (Fig. 4B).

The V1 loop of the TF virus (34 residues) was longer than the average V1 length of 28 residues (range, 11 to 64) of HIV-1 Env sequences found in the Los Alamos Sequence Database (26). As observed for heterologous neutralization, DH270 lineage antibodies acquired the ability to neutralize larger fractions of autologous viruses as maturation progressed by gaining activity for viruses with longer V1 loops, although at the expense of lower potency (fig. S14, A to C). This correlation was less clear for gp120 binding (fig. S14, D to F), however, suggesting that the V1 loop length dependency of V3-glycan bnAb neutralization has a conformational component. Thus, DH475 cooperated with the DH270 bnAb lineage by selecting viral escape mutants sensitive to bnAb lineage members.

For DH272, the viral variants that we made did not implicate a specific cooperating escape mutation. The Δ134–143 (V1 deletion) mutated virus remained sensitive to DH272 neutralization; both combinations of the V1 deletion in our panel that were resistant to DH272 and sensitive to DH270.1 included D185N, which also caused DH272 resistance on its own but did not lead to DH270.1 sensitivity (Fig. 4C). Thus, we have suggestive, but not definitive, evidence that DH272 also participated in selecting escape mutants for the DH270 bnAb lineage.

Structure of DH270 lineage members

We determined crystal structures for the single-chain variable fragment of DH270.1 and the Fabs of DH270.UCA3, DH270.3, DH270.5, and DH270.6, as well as DH272 (table S4). Because of uncertainty in the inferred sequence of the germline precursor (fig. S15, A and B), we also determined the structure of DH270.UCA1, which has a somewhat differently configured CDR H3 loop (fig. S15C); reconfiguration of this loop during early affinity maturation could account for the observed increase with respect to the UCA in heterologous neutralization by several intermediates. The variable domains of the DH270 antibodies superposed well, indicating that affinity maturation modulated the antibody-antigen interface without substantially changing the antibody conformation (Fig. 5A). Mutations accumulated at different positions for DH270 lineage bnAbs in distinct branches (fig. S16), possibly accounting for their distinct neutralization properties. DH272 had a CDR H3 configured differently from that of DH270 lineage members and a significantly longer CDR L1 (Fig. 5B), compatible with their distinct neutralization profiles.

We also compared the structures of DH270 lineage members with those of other N332-dependent bnAbs. All appear to have one long CDR loop that can extend through the network of glycans on the surface of the gp120 subunit and contact the “shielded” protein surface. The lateral surfaces of the Fab variable module can then interact with the

reconfigured or displaced glycans to either side. PGT128 has a long CDR H2 (Fig. 5C), in which a six-residue insertion is critical for neutralization breadth and potency (5, 17). PGT124 has a shorter and differently configured CDR H2 loop, but a long CDR H3 instead (Fig. 5D) (27).

Structure of the DH270–HIV-1 Env complex

We determined a three-dimensional image reconstruction, from negative-stain electron microscopy (EM), of the DH270.1 Fab bound with a gp140 trimer (92Br SOSIP.664) (Fig. 5, E and F, and fig. S17). The three DH270.1 Fabs project laterally, with their axes nearly normal to the threefold of gp140, in a distinctly more “horizontal” orientation than seen for PGT124, PGT135, and PGT128 (Fig. 5, G and H, and fig. S18). This orientational difference is consistent with differences between DH270 and PGT124 or PGT128 in the lengths and configurations of their CDR loops, which required an alternative DH270 bnAb position when docked onto the surface of the Env trimer. We docked the BG505 SOSIP coordinates (28) and the Fab into the EM reconstruction and further constrained the EM reconstruction image by the observed effects of BG505 SOSIP mutations in the gp140 surface image (figs. S17 and S19). Asp^{325} was essential for binding DH270.1 because it is a potential partner for Arg^{57} on the Fab. Mutating Asp^{321} led to a modest loss in affinity; R327A had no effect (fig. S20). These data further distinguish DH270 from PGT124 and PGT128. Individually mutating W101, Y105, D107, D115, Y116, or W117 in DH270.1 to alanine substantially reduced binding to the SOSIP trimer, as did pairwise mutation to the alanines of S106 and S109. The effects of these mutations illustrate the critical role of the CDR H3 loop in binding with HIV-1 Env (fig. S20).

DH270.UCA binding

The DH270.UCA did not bind to any of the 120 CH848 autologous gp120 Env glycoproteins isolated from time of infection to week 245 after infection, including the TF Env (Fig. 6A). DH270.UCA, as well as maturation intermediate antibodies, also did not recognize free glycans or cell surface membrane–expressed gp160 trimers (Fig. 6B). Conversely, the DH270.UCA bound to the Man_9-V3 synthetic glycopeptide mimic of the V3-glycan bnAb gp120 epitope (fig. S21A) and also bound to the aglycone form of the same peptide (fig. S21B). Similarly, the early intermediate antibodies (IA4, IA3, and IA2) each bound to both the Man_9-V3 glycopeptide and its aglycone form, and their binding was stronger to the aglycone V3 peptide than to the Man_9-V3 glycopeptide (fig. S21B). Overall, binding of the DH270.UCA and early intermediate antibodies to the Man_9-V3 glycopeptide was low (>10 μM) (fig. S21A). DH270.1 (V_H nucleotide mutation frequency, 5.6%) bound the glycopeptide with higher affinity than did the aglycone ($K_{d,glycopeptide}$ = 331 nM) (fig. S21, A and B), and as mutations accumulated, binding of the Man_9-V3 glycopeptide also increased, culminating in a K_d (apparent dissociation constant) of 188 nM in the most potent bnAb, DH270.6, which did not bind to the aglycone V3 peptide (fig. S21, A and B). Thus, both the Man_9-V3 glycopeptide and the aglycone V3 peptide bound to the DH270.UCA, and antibody binding was independent of glycans until the DH270 lineage had acquired a nucleotide mutation frequency of ~6%.

DISCUSSION

We can reconstruct from the data presented here a plausible series of events during the development of a V3-glycan bnAb in a natural infection. The DH272 and DH475 lineages neutralized the autologous TF and early viruses, and the resulting escape viruses were neutralized by the DH270 lineage. In particular, V1 deletions were necessary for neutralization of all but the most mature DH270 lineage antibodies. DH475 (and possibly DH272) escape variants stimulated DH270 affinity maturation, including both somatic mutations at sites of intrinsic mutability (11) and a crucial, improbable mutation at an AID cold spot within CDR H2 (G57R). The G57R mutation initiated expansion of the DH270 bnAb lineage. The low probability of this heterologous neutralization-conferring mutation and the complex lineage interactions that occurred is one explanation for why it took 4.5 years for the DH270 lineage to expand.

The CH848 viral population underwent a transition from a long V1 loop in the TF (34 residues) to short loops (16 to 17 residues) when escaping DH272/DH475 and facilitating expansion of DH270, to restoration of longer V1 loops later in infection as resistance to DH270 intermediates developed. Later DH270 antibodies adapted to viruses with longer V1 loops, allowing recognition of a broader spectrum of Envs and enhancing breadth. DH270.6 could neutralize heterologous viruses regardless of V1 loop length, but viruses with long loops tended to be less sensitive to it. Association of long V1 loops with reduced sensitivity was evident for three other V3-glycan bnAbs isolated from other individuals and may be a general feature of this class.

The V1 loop deletions in CH848 autologous virus removed the PNG site at position 137. Although the hypervariable nature of the V1 loop (which evolves by insertion and deletion, resulting in extreme length heterogeneity, as well as extreme variation in the number of PNG sites) complicates the interpretation of direct comparisons among unrelated HIV-1 strains, it is worth noting that a PNG site in this region specified as N137 was shown to be important for regulating affinity maturation of the PGT121 V3-glycan bnAb family, with some members of the lineage (PGT121 to PGT123) evolving to bind and others (PGT124) to accommodate or avoid this glycan (29).

Because we cannot foresee the susceptibility of each specific potential TF virus to a particular bnAb lineage it will be important for a vaccine to induce bnAbs against multiple epitopes on the HIV-1 Env to minimize TF virus escape (30, 31). In particular, induction of bnAb specificities beyond the HIV-1 V3-glycan epitope is critical for use in Asian populations where CRF01 strains (which, for the most part, lack the N332 PNG site required for efficient neutralization by V3-glycan bnAbs) are frequently observed.

Regarding what might have stimulated the UCA of the DH270 bnAb lineage the absence of detectable binding to the CH848 TF Env raised at least two possibilities. One is that the lineage arose at the end of year 1, either from a primary response to viruses present at that time (for example, with deletions in V1–V2) or from a subversion of an antibody lineage initially elicited by some other antigens. The other is that some altered form of the CH848 TF Env protein (for example, shed gp120, or a fragment of it) exposed the V3 loop and the

N301 and N332 glycans in a way that bound and stimulated the germline B cell receptor (BCR), although the native CH848 TF Env did not. Our findings suggest that a denatured, fragmented, or otherwise modified form of Env may have initiated the DH270 lineage. We cannot exclude that the DH270.UCA could not bind to autologous Env as an IgG but could potentially be triggered as an IgM BCR on a cell surface.

It will be important to define how often an improbable mutation such as G57R determines the time it takes for a bnAb lineage in an HIV-1–infected individual to develop and how many of the accompanying mutations are necessary for potency or breadth, rather than being nonessential mutations at AID mutational hotspots (11, 32). Mutations of the latter type might condition the outcome or modulate the impact of a key, improbable mutation, without contributing directly to affinity. Should the occurrence of an unlikely mutation be rate-limiting for breadth or potency in many other cases, a program of rational immunogen design will need to focus on modified Envs most likely to select very strongly for improbable yet critical antibody nucleotide changes.

The following proposal for a strategy for inducing V3-glycan bnAbs recreates the events that led to bnAb induction in CH848: starting by priming with a ligand that binds the bnAb UCA, such as the synthetic glycopeptide mimic of the V3-glycan bnAb gp120 epitope, and then boosting with an Env that can select G57R CDR H2 mutants, followed by Envs with progressive V1 lengths (fig. S22). We hypothesize that more direct targeting of V3-glycan UCAs and intermediate antibodies can accelerate the time of V3-glycan bnAb development in the setting of vaccination.

A limitation of this approach is that the selection of immunogens was based on the analysis of a single lineage from a single individual, and how frequently DH270-like lineages are present in the general population is unknown. Finally, our study describes a general strategy for the design of vaccine immunogens that can select specific antibody mutations, thereby directing antibody lineage maturation pathways.

MATERIAL AND METHODS

Study design

The CH848 donor, from which the DH270, DH272, and DH475 antibody lineages were isolated, is an African male enrolled in the CHAVI (Center for HIV/AIDS Vaccine Immunology) 001 acute HIV-1 infection cohort (33) and followed for 5 years, after which he started antiretroviral therapy. During this time, viral load ranged from 8927 to 442,749 copies/ml (median, 61,064 copies/ml), and CD4 counts ranged from 288 to 624 cells/mm^3 (median, 350 cells/mm^3). The time of infection was estimated by analyzing the sequence diversity in the first available sample using the Poisson-Fitter tool, as described in (10). Results were consistent with a single founder virus establishing the infection (34).

The mAbs DH270.1 and DH270.3 were isolated from cultured memory B cells isolated 205 weeks after transmission (14). The mAbs DH270.6 and DH475 were isolated from Man_9-V3 glycopeptide–specific memory B cells collected 232 and 234 weeks after transmission, respectively, using direct sorting. The mAbs DH270.2, DH270.4, and DH270.5 were

isolated from memory B cells collected 232 weeks after transmission that bound to Consensus C gp120 Env but not to Consensus C N332A gp120 Env, using direct sorting.

Experimental methods

Detailed description of experimental methods is provided in Supplementary Materials and Methods.

Statistical analyses

Statistical analysis was performed using R. The specific tests used to determine significance are reported for each instance in the text.

Supplementary Material

Refer to Web version on PubMed Central for supplementary material.

Acknowledgments

We thank the following for technical assistance: M. C. Mangiapani, R. J. Parks, C. Vivian, K. Lloyd, D. M. Kozink, F. Perrin, A. J. Cooper, A. Foulger, G. Hernandez, J. Pritchett, S. Arora, T. Gurley, L. Armand, A. Eaton, A. Wang, and the Duke Human Vaccine Institute (DHVI) Flow Core Facility from DHVI; G. H. Learn, T. G. Decker, and Y. Li from the University of Pennsylvania; N. Tumba from the National Institute for Communicable Diseases (Johannesburg); the beamline staff at 24-ID-C and 24-ID-E of the Advanced Photon Source, and the Harvard Medical School EM staff. We also thank K. Soderberg (DHVI) for project management and the HIV Vaccine Trials Network for the continued use of NGS prevaccination samples from the HVTN082 and HVTN204 trials (35).

Funding: E.F.K. and R.R.M. are supported by the F30 Ruth L. Kirschstein National Research Service Award (AI112426 and AI122982-0, respectively). D.F. is supported by an F32 fellowship (1F32AI116355-01) from the NIH. R.R.M. is supported by a Medical Scientist Training Program grant (T32GM007171). K.O.S. is supported by a National Institute of Allergy and Infectious Diseases (NIAID) grant (R01-AI120801). This work was funded by UM1 AI100645 from the Duke CHAVI–Immunogen Discovery, Division of AIDS, NIAID, NIH (to B.F.H.).

REFERENCES AND NOTES

1. Burton DR, Mascola JR. Antibody responses to envelope glycoproteins in HIV-1 infection. Nat Immunol. 2015; 16:571–576. [PubMed: 25988889]
2. Mascola JR, Haynes BF. HIV-1 neutralizing antibodies: Understanding nature's pathways. Immunol Rev. 2013; 254:225–244. [PubMed: 23772623]
3. Walker LM, Huber M, Doores KJ, Falkowska E, Pejchal R, Julien JP, Wang SK, Ramos A, Chan-Hui PY, Moyle M, Mitcham JL, Hammond PW, Olsen OA, Phung P, Fling S, Wong CH, Phogat S, Wrin T, Simek MD, Koff WC, Wilson IA, Burton DR, Poignard P. Broad neutralization coverage of HIV by multiple highly potent antibodies. Nature. 2011; 477:466–470. [PubMed: 21849977]
4. Walker LM, Phogat SK, Chan-Hui PY, Wagner D, Phung P, Goss JL, Wrin T, Simek MD, Fling S, Mitcham JL, Lehrman JK, Priddy FH, Olsen OA, Frey SM, Hammond PW, Kaminsky S, Zamb T, Moyle M, Koff WC, Poignard P, Burton DR. Broad and potent neutralizing antibodies from an African donor reveal a new HIV-1 vaccine target. Science. 2009; 326:285–289. [PubMed: 19729618]
5. Doores KJ, Kong L, Krumm SA, Le KM, Sok D, Laserson U, Garces F, Poignard P, Wilson IA, Burton DR. Two classes of broadly neutralizing antibodies within a single lineage directed to the high-mannose patch of HIV envelope. J Virol. 2015; 89:1105–1118. [PubMed: 25378488]
6. Sok D, Doores KJ, Briney B, Le KM, Saye-Francisco KL, Ramos A, Kulp DW, Julien JP, Menis S, Wickramasinghe L, Seaman MS, Schief WR, Wilson IA, Poignard P, Burton DR. Promiscuous glycan site recognition by antibodies to the high-mannose patch of gp120 broadens neutralization of HIV. Sci Transl Med. 2014; 6:236ra263.

7. Sok D, Laserson U, Laserson J, Liu Y, Vigneault F, Julien JP, Briney B, Ramos A, Saye KF, Le K, Mahan A, Wang S, Kardar M, Yaari G, Walker LM, Simen BB, St John EP, Chan-Hui PY, Swiderek K, Kleinstein SH, Alter G, Seaman MS, Chakraborty AK, Koller D, Wilson IA, Church GM, Burton DR, Poignard P. The effects of somatic hypermutation on neutralization and binding in the PGT121 family of broadly neutralizing HIV antibodies. PLOS Pathog. 2013; 9:e1003754. [PubMed: 24278016]
8. Mouquet H, Scharf L, Euler Z, Liu Y, Eden C, Scheid JF, Halper-Stromberg A, Gnanapragasam PNP, Spencer DIR, Seaman MS, Schuitemaker H, Feizi T, Nussenzweig MC, Bjorkman PJ. Complex-type N-glycan recognition by potent broadly neutralizing HIV antibodies. Proc Natl Acad Sci USA. 2012; 109:E3268–E3277. [PubMed: 23115339]
9. Haynes BF, Kelsoe G, Harrison SC, Kepler TB. B-cell–lineage immunogen design in vaccine development with HIV-1 as a case study. Nat Biotechnol. 2012; 30:423–433. [PubMed: 22565972]
10. Liao H-X, Lynch R, Zhou T, Gao F, Alam SM, Boyd SD, Fire AZ, Roskin KM, Schramm CA, Zhang Z, Zhu J, Shapiro L, NISC Comparative Sequencing Program. Mullikin JC, Gnanakaran S, Hraber P, Wiehe K, Kelsoe G, Yang G, Xia S-M, Montefiori DC, Parks R, Lloyd KE, Scearce RM, Soderberg KA, Cohen M, Kamanga G, Louder MK, Tran LM, Chen Y, Cai F, Chen S, Moquin S, Du X, Joyce MG, Srivatsan S, Zhang B, Zheng A, Shaw GM, Hahn BH, Kepler TB, Korber BTM, Kwong PD, Mascola JR, Haynes BF. Co-evolution of a broadly neutralizing HIV-1 antibody and founder virus. Nature. 2013; 496:469–476. [PubMed: 23552890]
11. Bonsignori M, Zhou T, Sheng Z, Chen L, Gao F, Joyce MG, Ozorowski G, Chuang G-Y, Schramm CA, Wiehe K, Alam SM, Bradley T, Gladden MA, Hwang KK, Iyengar S, Kumar A, Lu X, Luo K, Mangiapani MC, Parks RJ, Song H, Acharya P, Bailer RT, Cao A, Druz A, Georgiev IS, Kwon YD, Louder MK, Zhang B, Zheng A, Hill BJ, Kong R, Soto C, NISC Comparative Sequencing Program. Mullikin JC, Douek DC, Montefiori DC, Moody MA, Shaw GM, Hahn BH, Kelsoe G, Hraber PT, Korber BT, Boyd SD, Fire AZ, Kepler TB, Shapiro L, Ward AB, Mascola JR, Liao H-X, Kwong PD, Haynes BF. Maturation pathway from germline to broad HIV-1 neutralizer of a CD4-mimic antibody. Cell. 2016; 165:449–463. [PubMed: 26949186]
12. Gao F, Bonsignori M, Liao HX, Kumar A, Xia SM, Lu X, Cai F, Hwang KK, Song H, Zhou T, Lynch RM, Alam SM, Moody MA, Ferrari G, Berrong M, Kelsoe G, Shaw GM, Hahn BH, Montefiori DC, Kamanga G, Cohen MS, Hraber P, Kwong PD, Korber BT, Mascola JR, Kepler TB, Haynes BF. Cooperation of B cell lineages in induction of HIV-1-broadly neutralizing antibodies. Cell. 2014; 158:481–491. [PubMed: 25065977]
13. Pancera M, Zhou T, Druz A, Georgiev IS, Soto C, Gorman J, Huang J, Acharya P, Chuang GY, Ofek G, Stewart-Jones GBE, Stuckey J, Bailer RT, Joyce MG, Louder MK, Tumba N, Yang Y, Zhang B, Cohen MS, Haynes BF, Mascola JR, Morris L, Munro JB, Blanchard SC, Mothes W, Connors M, Kwong PD. Structure and immune recognition of trimeric pre-fusion HIV-1 Env. Nature. 2014; 514:455–461. [PubMed: 25296255]
14. Bonsignori M, Hwang K-K, Chen X, Tsao C-Y, Morris L, Gray E, Marshall DJ, Crump JA, Kapiga SH, Sam NE, Sinangil F, Pancera M, Yongping Y, Zhang B, Zhu J, Kwong PD, O'Dell S, Mascola JR, Wu L, Nabel GJ, Phogat S, Seaman MS, Whitesides JF, Moody MA, Kelsoe G, Yang X, Sodroski J, Shaw GM, Montefiori DC, Kepler TB, Tomaras GD, Alam SM, Liao H-X, Haynes BF. Analysis of a clonal lineage of HIV-1 envelope V2/V3 conformational epitope-specific broadly neutralizing antibodies and their inferred unmutated common ancestors. J Virol. 2011; 85:9998–10009. [PubMed: 21795340]
15. Gray ES, Moody MA, Wibmer CK, Chen X, Marshall D, Amos J, Moore PL, Foulger A, Yu J-S, Lambson B, Abdool Karim S, Whitesides J, Tomaras GD, Haynes BF, Morris L, Liao H-X. Isolation of a monoclonal antibody that targets the α-2 helix of gp120 and represents the initial autologous neutralizing-antibody response in an HIV-1 subtype C-infected individual. J Virol. 2011; 85:7719–7729. [PubMed: 21613396]
16. Alam SM, Aussedat B, Vohra Y, Meyerhoff RR, Cale EM, Walkowicz WE, Radakovich NA, Armand L, Parks R, Sutherland L, Scearce R, Joyce MG, Pancera M, Druz A, Georgiev I, Von Holle T, Eaton A, Fox C, Reed SG, Louder MK, Bailer RT, Morris L, Abdool Karim S, Cohen M, Liao HX, Montefiori D, Park PK, Fernandez-Tejada A, Wiehe K, Santra S, Kepler TB, Saunders KO, Sodroski J, Kwong PD, Mascola JR, Bonsignori M, Moody MA, Danishefsky SJ, Haynes BF. Mimicry of an HIV broadly neutralizing antibody epitope with a synthetic glycopeptide. Sci Transl Med. 2017; 9:eaai7521. [PubMed: 28298421]

17. Pejchal R, Doores KJ, Walker LM, Khayat R, Huang PS, Wang SK, Stanfield RL, Julien JP, Ramos A, Crispin M, Depetris R, Katpally U, Marozsan A, Cupo A, Maloveste S, Liu Y, McBride R, Ito Y, Sanders RW, Ogohara C, Paulson JC, Feizi T, Scanlan CN, Wong CH, Moore JP, Olson WC, Ward AB, Poignard P, Schief WR, Burton DR, Wilson IA. A potent and broad neutralizing antibody recognizes and penetrates the HIV glycan shield. Science. 2011; 334:1097–1103. [PubMed: 21998254]

18. Aussedat B, Vohra Y, Park PK, Fernández-Tejada A, Alam SM, Dennison SM, Jaeger FH, Anasti K, Stewart S, Blinn JH, Liao H-X, Sodroski JG, Haynes BF, Danishefsky SJ. Chemical synthesis of highly congested gp120 V1V2 N-glycopeptide antigens for potential HIV-1-directed vaccines. J Am Chem Soc. 2013; 135:13113–13120. [PubMed: 23915436]

19. Alam SM, Dennison SM, Aussedat B, Vohra Y, Park PK, Fernández-Tejada A, Stewart S, Jaeger FH, Anasti K, Blinn JH, Kepler TB, Bonsignori M, Liao H-X, Sodroski JG, Danishefsky SJ, Haynes BF. Recognition of synthetic glycopeptides by HIV-1 broadly neutralizing antibodies and their unmutated ancestors. Proc Natl Acad Sci USA. 2013; 110:18214–18219. [PubMed: 24145434]

20. Yaari G, Van der Heiden JA, Uduman M, Gadala-Maria D, Gupta N, Stern JNH, O'Connor KC, Hafler DA, Laserson U, Vigneault F, Kleinstein SH. Models of somatic hypermutation targeting and substitution based on synonymous mutations from high-throughput immunoglobulin sequencing data. Front Immunol. 2013; 4:358. [PubMed: 24298272]

21. We accessed the SF5 mutability model dataset at http://clip.med.yale.edu/shm/download.php

22. Kong L, Lee JH, Doores KJ, Murin CD, Julien JP, McBride R, Liu Y, Marozsan A, Cupo A, Klasse PJ, Hoffenberg S, Caulfield M, King CR, Hua Y, Le KM, Khayat R, Deller MC, Clayton T, Tien H, Feizi T, Sanders RW, Paulson JC, Moore JP, Stanfield RL, Burton DR, Ward AB, Wilson IA. Supersite of immune vulnerability on the glycosylated face of HIV-1 envelope glycoprotein gp120. Nat Struct Mol Biol. 2013; 20:796–803. [PubMed: 23708606]

23. Julien JP, Sok D, Khayat R, Lee JH, Doores KJ, Walker LM, Ramos A, Diwanji DC, Pejchal R, Cupo A, Katpally U, Depetris RS, Stanfield RL, McBride R, Marozsan AJ, Paulson JC, Sanders RW, Moore JP, Burton DR, Poignard P, Ward AB, Wilson IA. Broadly neutralizing antibody PGT121 allosterically modulates CD4 binding via recognition of the HIV-1 gp120 V3 base and multiple surrounding glycans. PLOS Pathog. 2013; 9:e1003342. [PubMed: 23658524]

24. Pancera M, Yang Y, Louder MK, Gorman J, Lu G, McLellan JS, Stuckey J, Zhu J, Burton DR, Koff WC, Mascola JR, Kwong PD. N332-directed broadly neutralizing antibodies use diverse modes of HIV-1 recognition: Inferences from heavy-light chain complementation of function. PLOS ONE. 2013; 8:e55701. [PubMed: 23431362]

25. Moore PL, Gray ES, Wibmer CK, Bhiman JN, Nonyane M, Sheward DJ, Hermanus T, Bajimaya S, Tumba NL, Abrahams M-R, Lambson BE, Ranchobe N, Ping L, Ngandu N, Abdool Karim Q, Abdool Karim SS, Swanstrom RI, Seaman MS, Williamson C, Morris L. Evolution of an HIV glycan–dependent broadly neutralizing antibody epitope through immune escape. Nat Med. 2012; 18:1688–1692. [PubMed: 23086475]

26. Los Alamos National Laboratory (LANL). HIV sequence database (LANL, 2016). www.hiv.lanl.gov/content/sequence/HIV/mainpage.html

27. Garces F, Sok D, Kong L, McBride R, Kim HJ, Saye-Francisco KF, Julien JP, Hua Y, Cupo A, Moore JP, Paulson JC, Ward AB, Burton DR, Wilson IA. Structural evolution of glycan recognition by a family of potent HIV antibodies. Cell. 2014; 159:69–79. [PubMed: 25259921]

28. Lee JH, de Val N, Lyumkis D, Ward AB. Model building and refinement of a natively glycosylated HIV-1 Env protein by high-resolution cryoelectron microscopy. Structure. 2015; 23:1943–1951. [PubMed: 26388028]

29. Garces F, Lee JH, de Val N, de la Pena AT, Kong L, Puchades C, Hua Y, Stanfield RL, Burton DR, Moore JP, Sanders RW, Ward AB, Wilson IA. Affinity maturation of a potent family of HIV antibodies is primarily focused on accommodating or avoiding glycans. Immunity. 2015; 43:1053–1063. [PubMed: 26682982]

30. Bonsignori M, Montefiori DC, Wu X, Chen X, Hwang KK, Tsao CY, Kozink DM, Parks RJ, Tomaras GD, Crump JA, Kapiga SH, Sam NE, Kwong PD, Kepler TB, Liao HX, Mascola JR, Haynes BF. Two distinct broadly neutralizing antibody specificities of different clonal lineages in a

single HIV-1-infected donor: Implications for vaccine design. J Virol. 2012; 86:4688–4692. [PubMed: 22301150]

31. Wagh K, Bhattacharya T, Williamson C, Robles A, Bayne M, Garrity J, Rist M, Rademeyer C, Yoon H, Lapedes A, Gao H, Greene K, Louder MK, Kong R, Abdool Karim S, Burton DR, Barouch DH, Nussenzweig MC, Mascola JR, Morris L, Montefiori DC, Korber B, Seaman MS. Optimal combinations of broadly neutralizing antibodies for prevention and treatment of HIV-1 clade C infection. PLOS Pathog. 2016; 12:e1005520. [PubMed: 27028935]
32. Yeap L-S, Hwang JK, Du Z, Meyers RM, Meng F-L, Jakubauskaitė A, Liu M, Mani V, Neuberg D, Kepler TB, Wang JH, Alt FW. Sequence-intrinsic mechanisms that target aid mutational outcomes on antibody genes. Cell. 2015; 163:1124–1137. [PubMed: 26582132]
33. Tomaras GD, Yates NL, Liu P, Qin L, Fouda GG, Chavez LL, Decamp AC, Parks RJ, Ashley VC, Lucas JT, Cohen M, Eron J, Hicks CB, Liao HX, Self SG, Landucci G, Forthal DN, Weinhold KJ, Keele BF, Hahn BH, Greenberg ML, Morris L, Karim SS, Blattner WA, Montefiori DC, Shaw GM, Perelson AS, Haynes BF. Initial B-cell responses to transmitted human immunodeficiency virus type 1: Virion-binding immunoglobulin M (IgM) and IgG antibodies followed by plasma anti-gp41 antibodies with ineffective control of initial viremia. J Virol. 2008; 82:12449–12463. [PubMed: 18842730]
34. Shaw GM, Hunter E, HIV transmission. Cold Spring Harb Perspect Med. 2012; 2:a006965. [PubMed: 23043157]
35. Williams WB, Liao HX, Moody MA, Kepler TB, Alam SM, Gao F, Wiehe K, Trama AM, Jones K, Zhang R, Song H, Marshall DJ, Whitesides JF, Sawatzki K, Hua A, Liu P, Tay MZ, Seaton KE, Shen X, Foulger A, Lloyd KE, Parks R, Pollara J, Ferrari G, Yu JS, Vandergrift N, Montefiori DC, Sobieszczyk ME, Hammer S, Karuna S, Gilbert P, Grove D, Grunenberg N, McElrath MJ, Mascola JR, Koup RA, Corey L, Nabel GJ, Morgan C, Churchyard G, Maenza J, Keefer M, Graham BS, Baden LR, Tomaras GD, Haynes BF. Diversion of HIV-1 vaccine–induced immunity by gp41-microbiota cross-reactive antibodies. Science. 2015; 349:aab1253. [PubMed: 26229114]
36. Kepler TB. Reconstructing a B-cell clonal lineage. I. Statistical inference of unobserved ancestors. F1000Res. 2013; 2:103. [PubMed: 24555054]
37. Cowell LG, Kepler TB. The nucleotide-replacement spectrum under somatic hypermutation exhibits microsequence dependence that is strand-symmetric and distinct from that under germline mutation. J Immunol. 2000; 164:1971–1976. [PubMed: 10657647]
38. Betz AG, Rada C, Pannell R, Milstein C, Neuberger MS. Passenger transgenes reveal intrinsic specificity of the antibody hypermutation mechanism: Clustering, polarity, and specific hot spots. Proc Natl Acad Sci USA. 1993; 90:2385–2388. [PubMed: 8460148]
39. Bransteitter R, Pham P, Calabrese P, Goodman MF. Biochemical analysis of hypermutational targeting by wild type and mutant activation-induced cytidine deaminase. J Biol Chem. 2004; 279:51612–51621. [PubMed: 15371439]
40. Seaman MS, Janes H, Hawkins N, Grandpre LE, Devoy C, Giri A, Coffey RT, Harris L, Wood B, Daniels MG, Bhattacharya T, Lapedes A, Polonis VR, McCutchan FE, Gilbert PB, Self SG, Korber BT, Montefiori DC, Mascola JR. Tiered categorization of a diverse panel of HIV-1 Env pseudoviruses for assessment of neutralizing antibodies. J Virol. 2010; 84:1439–1452. [PubMed: 19939925]
41. Salazar-Gonzalez JF, Salazar MG, Keele BF, Learn GH, Giorgi EE, Li H, Decker JM, Wang S, Baalwa J, Kraus MH, Parrish NF, Shaw KS, Guffey MB, Bar KJ, Davis KL, Ochsenbauer-Jambor C, Kappes JC, Saag MS, Cohen MS, Mulenga J, Derdeyn CA, Allen S, Hunter E, Markowitz M, Hraber P, Perelson AS, Bhattacharya T, Haynes BF, Korber BT, Hahn BH, Shaw GM. Genetic identity, biological phenotype, and evolutionary pathways of transmitted/founder viruses in acute and early HIV-1 infection. J Exp Med. 2009; 206:1273–1289. [PubMed: 19487424]
42. Keele BF, Giorgi EE, Salazar-Gonzalez JF, Decker JM, Pham KT, Salazar MG, Sun C, Grayson T, Wang S, Li H, Wei X, Jiang C, Kirchherr JL, Gao F, Anderson JA, Ping LH, Swanstrom R, Tomaras GD, Blattner WA, Goepfert PA, Kilby JM, Saag MS, Delwart EL, Busch MP, Cohen MS, Montefiori DC, Haynes BF, Gaschen B, Athreya GS, Lee HY, Wood N, Seoighe C, Perelson AS, Bhattacharya T, Korber BT, Hahn BH, Shaw GM. Identification and characterization of transmitted and early founder virus envelopes in primary HIV-1 infection. Proc Natl Acad Sci USA. 2008; 105:7552–7557. [PubMed: 18490657]

43. Hraber P, Korber B, Wagh K, Giorgi EE, Bhattacharya T, Gnanakaran S, Lapedes AS, Learn GH, Kreider EF, Li Y, Shaw GM, Hahn BH, Montefiori DC, Alam SM, Bonsignori M, Moody MA, Liao HX, Gao F, Haynes BF. Longitudinal Antigenic Sequences and Sites from Intra-Host Evolution (LASSIE) identifies immune-selected HIV variants. Viruses. 2015; 7:5443–5475. [PubMed: 26506369]
44. Kirchherr JL, Lu X, Kasongo W, Chalwe V, Mwananyanda L, Musonda RM, Xia SM, Scearce RM, Liao HX, Montefiori DC, Haynes BF, Gao F. High throughput functional analysis of HIV-1 env genes without cloning. J Virol Methods. 2007; 143:104–111. [PubMed: 17416428]
45. Go EP, Herschhorn A, Gu C, Castillo-Menendez L, Zhang S, Mao Y, Chen H, Ding H, Wakefield JK, Hua D, Liao HX, Kappes JC, Sodroski J, Desaire H. Comparative analysis of the glycosylation profiles of membrane-anchored HIV-1 envelope glycoprotein trimers and soluble gp140. J Virol. 2015; 89:8245–8257. [PubMed: 26018173]
46. Fera D, Schmidt AG, Haynes BF, Gao F, Liao HX, Kepler TB, Harrison SC. Affinity maturation in an HIV broadly neutralizing B-cell lineage through reorientation of variable domains. Proc Natl Acad Sci USA. 2014; 111:10275–10280. [PubMed: 24982157]
47. Zhou T, Zhu J, Wu X, Moquin S, Zhang B, Acharya P, Georgiev IS, Altae-Tran HR, Chuang G-Y, Joyce MG, Kwon YD, Longo NS, Louder MK, Luongo T, McKee K, Schramm CA, Skinner J, Yang Y, Yang Z, Zhang Z, Zheng A, Bonsignori M, Haynes BF, Scheid JF, Nussenzweig MC, Simek M, Burton DR, Koff WC, NISC Comparative Sequencing Program. Mullikin JC, Connors M, Shapiro L, Nabel GJ, Mascola JR, Kwong PD. Multidonor analysis reveals structural elements, genetic determinants, and maturation pathway for HIV-1 neutralization by VRC01-class antibodies. Immunity. 2013; 39:245–258. [PubMed: 23911655]
48. Sanders RW, Derking R, Cupo A, Julien J-P, Yasmeen A, Val Nde, Kim HJ, Blattner C, de la Peña AT, Korzun J, Golabek M, de Los Reyes K, Ketas TJ, van Gils MJ, King CR, Wilson IA, Ward AB, Klasse PJ, Moore JP. A next-generation cleaved, soluble HIV-1 Env trimer, BG505 SOSIP.664 gp140, expresses multiple epitopes for broadly neutralizing but not non-neutralizing antibodies. PLOS Pathog. 2013; 9:e1003618. [PubMed: 24068931]
49. Nickle DC, Heath L, Jensen MA, Gilbert PB, Mullins JI, Kosakovsky Pond SL. HIV-specific probabilistic models of protein evolution. PLOS ONE. 2007; 2:e503. [PubMed: 17551583]
50. Gnanakaran S, Daniels MG, Bhattacharya T, Lapedes AS, Sethi A, Li M, Tang H, Greene K, Gao H, Haynes BF, Cohen MS, Shaw GM, Seaman MS, Kumar A, Gao F, Montefiori DC, Korber B. Genetic signatures in the envelope glycoproteins of HIV-1 that associate with broadly neutralizing antibodies. PLOS Comput Biol. 2010; 6:e1000955. [PubMed: 20949103]
51. Bhattacharya T, Daniels M, Heckerman D, Foley B, Frahm N, Kadie C, Carlson J, Yusim K, McMahon B, Gaschen B, Mallal S, Mullins JI, Nickle DC, Herbeck J, Rousseau C, Learn GH, Miura T, Brander C, Walker B, Korber B. Founder effects in the assessment of HIV polymorphisms and HLA allele associations. Science. 2007; 315:1583–1586. [PubMed: 17363674]
52. Kong L, Torrents de la Peña A, Deller MC, Garces F, Sliepen K, Hua Y, Stanfield RL, Sanders RW, Wilson IA. Complete epitopes for vaccine design derived from a crystal structure of the broadly neutralizing antibodies PGT128 and 8ANC195 in complex with an HIV-1 Env trimer. Acta Crystallogr D Biol Crystallogr. 2015; 71:2099–2108. [PubMed: 26457433]

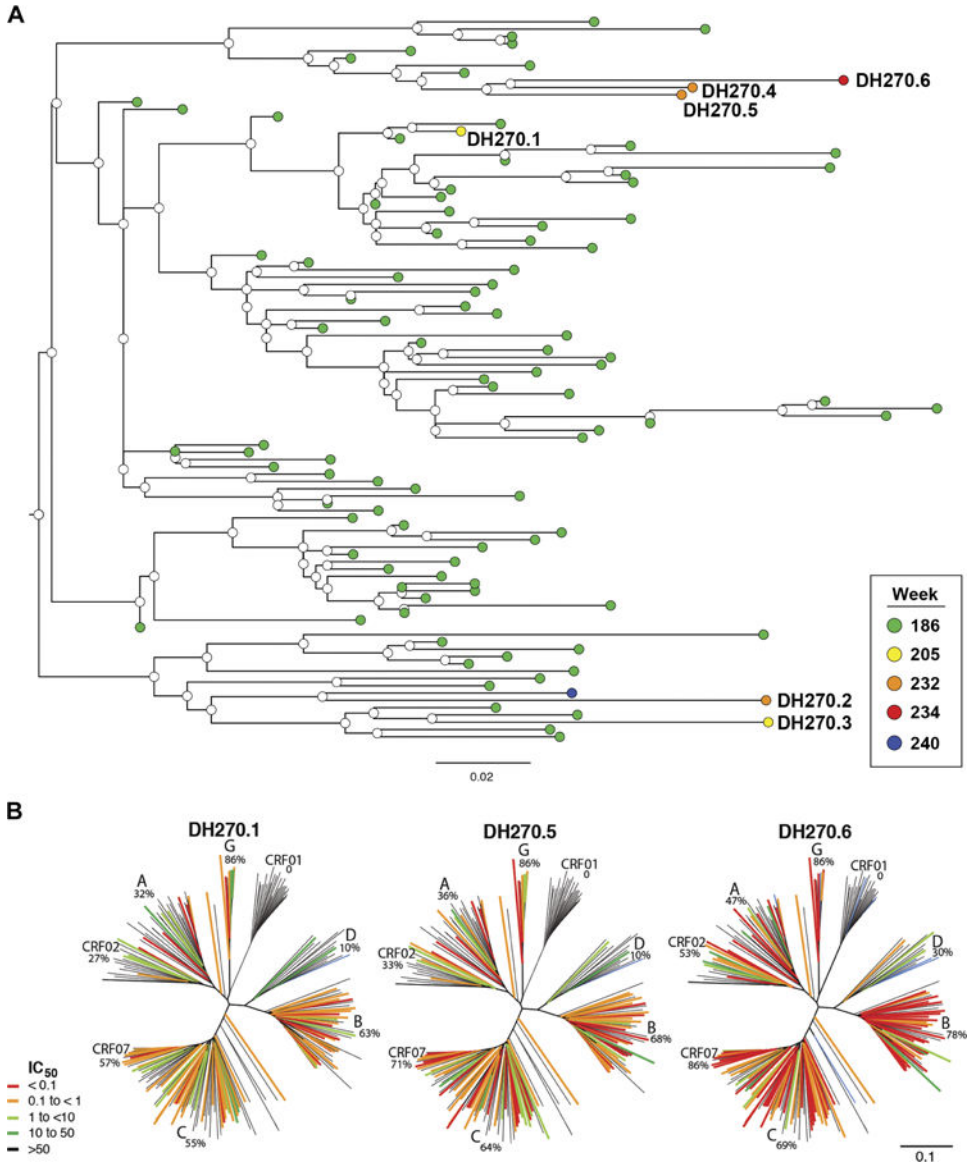

Fig. 1. DH270 lineage with time of appearance and neutralization by selected members

(**A**) Phylogenetic relationship of six monoclonal antibodies (mAbs) and 93 NGS $V_H(D)J_H$ sequence reads in the DH270 clonal lineage. External nodes (filled circles) represent $V_H(D)J_H$ nucleotide sequences of either antibodies retrieved from cultured and sorted memory B cells (labeled) or a curated data set of NGS $V_H(D)J_H$ rearrangement reads (unlabeled). Coloring is by time of isolation. Samples from weeks 11, 19, 64, 111, 160, 186, and 240 were tested, and time points from which no NGS reads within the lineage were retrieved are reported in table S2. Internal nodes (open circles) represent inferred ancestral intermediate sequences. Units for branch-length estimates are nucleotide substitution per site. (**B**) Neutralization dendrograms display single mAb neutralization of a genetically diverse panel of 207 HIV-1 isolates. Coloring is by median inhibitory concentration (IC_{50}). See also data set S1.

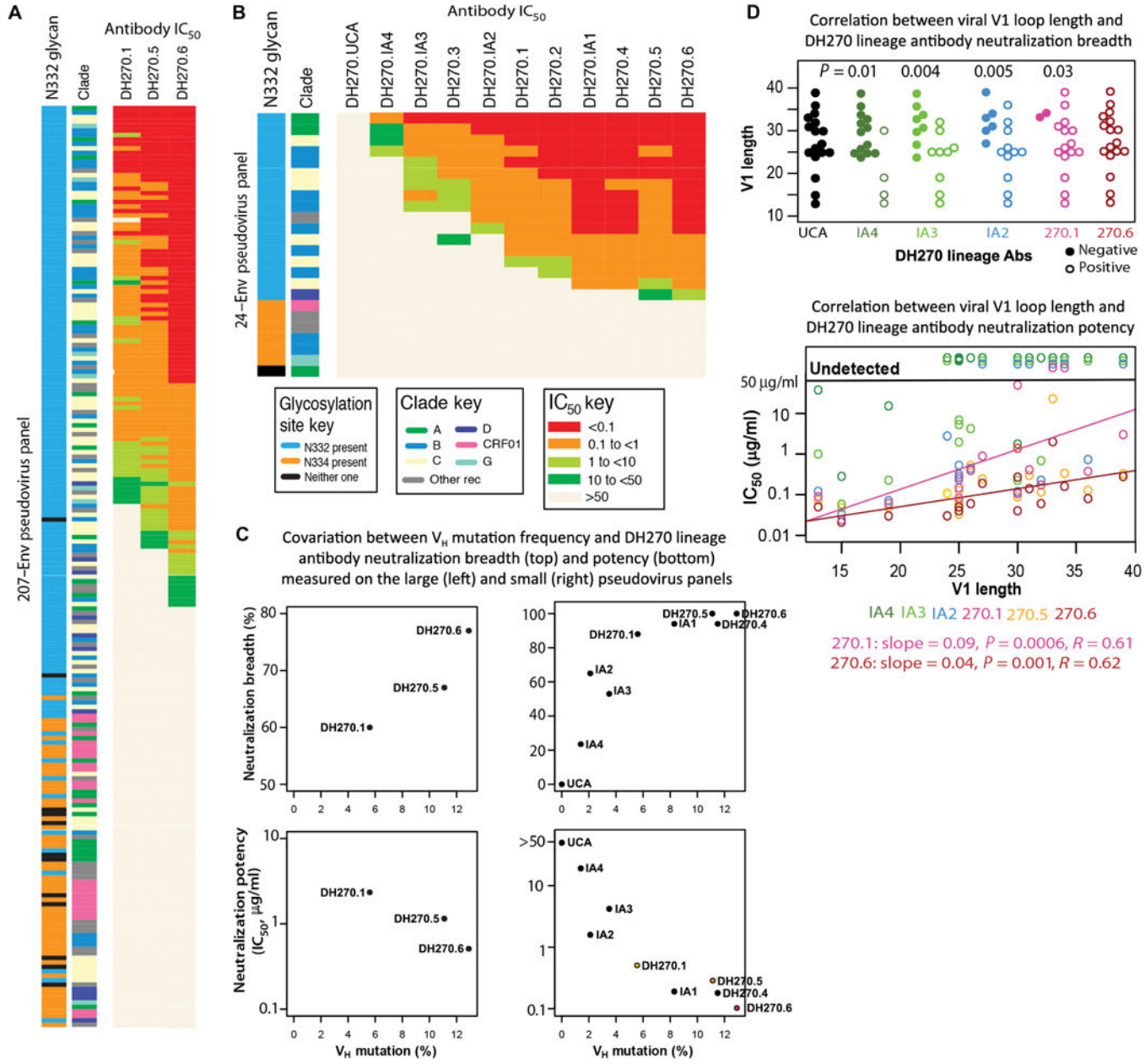

Fig. 2. Heterologous breadth in the DH270 lineage

(**A**) Neutralizing activity of DH270.1, DH270.5, and DH270.6 bnAbs (columns) for 207 tier 2 heterologous viruses (rows). Coloring is by neutralization IC_{50} (in µg/ml). The first column displays the presence of a PNG site at position 332 (blue), at N334 (orange), or at neither one (black). The second column indicates the clade of each individual HIV-1 strain and is color-coded as indicated: clade A, green; clade B, blue; clade C, yellow; clade D, purple; CRF01, pink; clade G, cyan; others, gray. See data set S1. (**B**). Heterologous neutralization of all DH270 lineage antibodies for a 24-virus panel. Color coding for the presence of PNG sites, clade, and IC_{50} is the same as in (A). See fig. S1 and data set S3. (**C**) Covariation between V_H mutation frequencies (*x* axis), neutralization breadth (*y* axis, top), and potency (*y* axis, bottom) of individual antibodies against viruses with a PNG site at

position N332 from the larger (left) and smaller (right) pseudovirus panels. (**D**) Correlation between viral V1 loop length and DH270 lineage antibody neutralization. Top: Neutralization of 17 viruses (with N332; sensitive to at least one DH270 lineage antibody) by selected DH270 lineage antibodies from unmutated common ancestor (UCA) to mature bnAbs (*x* axis). Viruses are identified by their respective V1 loop lengths (*y* axis); for each virus, neutralization sensitivity is indicated by an open circle, and resistance is indicated by a solid circle. The *P* value is a Wilcoxon rank sum comparison of V1 length distributions between sensitive and resistant viruses. Bottom: Regression lines (IC_{50} for neutralization versus V1 loop length) for DH270.1 and DH270.6, with a *P* value based on Kendall's τ.

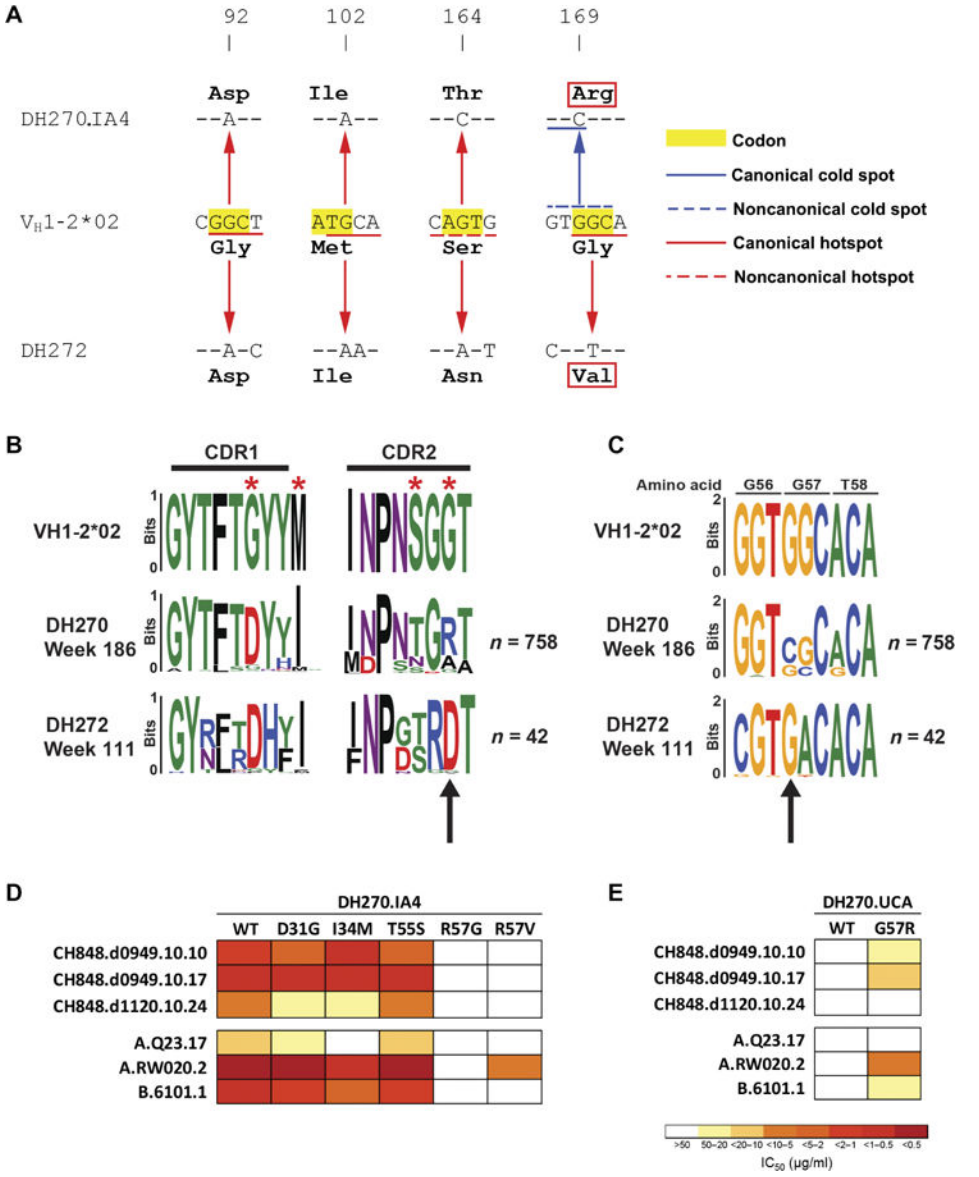

Fig. 3. A single disfavored mutation early during DH270 clonal development conferred neutralizing activity on the V3-glycan bnAb DH270 precursor antibodies

(**A**) Nucleotide alignment of DH270.IA4 and DH272 to *V_H1–2*02* sequence at the four V_H positions that mutated from DH270.UCA to DH270.IA4. The mutated codons are highlighted in yellow. AID hotspots are indicated by red lines (solid, canonical; dashed, noncanonical); AID cold spots are indicated by blue lines (solid, canonical; dashed, noncanonical) (20). At position 169, DH270.IA4 retained positional conformity with DH272 but not identity conformity (red boxes). (**B**) Sequence logo plot of amino acids mutated from germline (top) in the NGS reads of the DH270 (middle) and DH272 (bottom) lineages at weeks 186 and 111 after transmission, respectively. Red asterisks indicate amino acids mutated in DH270.IA4. The black arrow indicates lack of identity conformity between the two lineages at amino acid position 57. (**C**) Sequence logo plot of nucleotide mutations (positions 165 to 173) in the DH270 and DH272 lineages at weeks 186 and 111 after

transmission, respectively. The arrow indicates position 169. (**D**) Effect of reversion mutations on DH270.IA4 neutralization. Coloring is by IC_{50}. WT, wild type. (**E**) Effect of G57R mutation on DH270.UCA auto-logous (top) and heterologous (bottom) neutralizing activity.

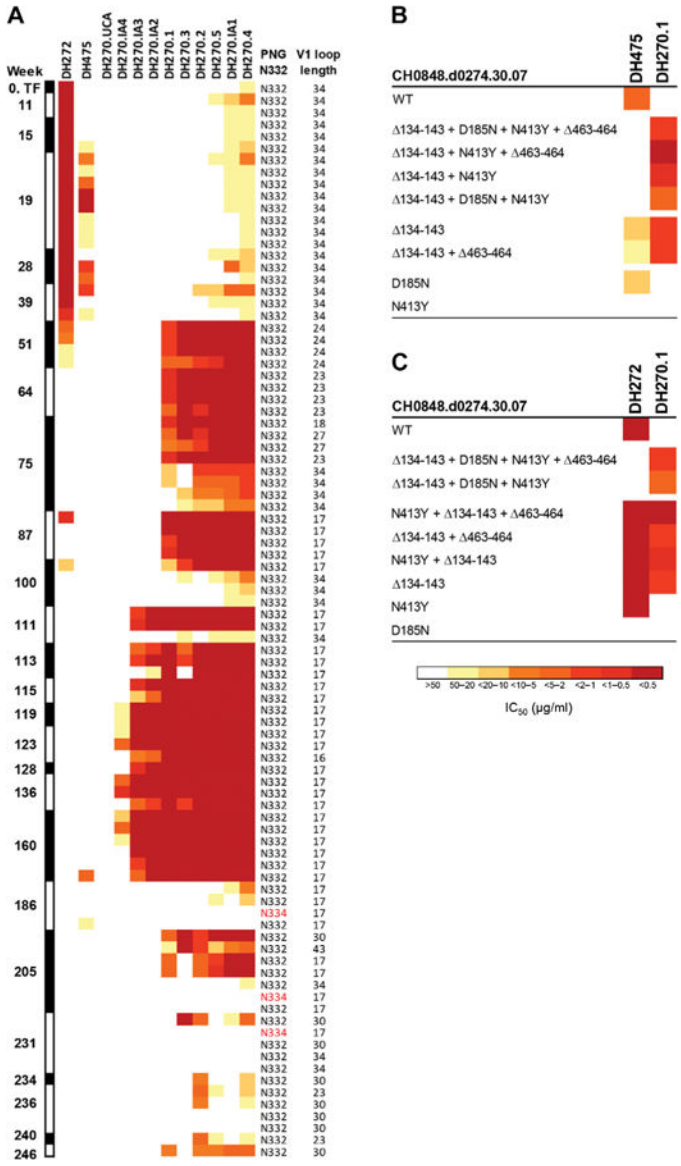

Fig. 4. Cooperation among DH270, DH272, and DH475 N332-dependent V3-glycan neutralizing antibody lineages

(**A**) Neutralizing activity of DH272, DH475, and DH270 lineage antibodies (columns) against 90 autologous viruses isolated from CH848 over time (rows). Neutralization potency (IC_{50}) is shown as indicated in the bar. For each pseudovirus, presence of a PNG site at N332 or N334, and V1 loop length are indicated in the right columns. See also data set S2. (**B** and **C**) Susceptibility of autologous viruses bearing selected immunotype-specific mutations to DH270.1 and to DH475 (B) or DH272 (C).

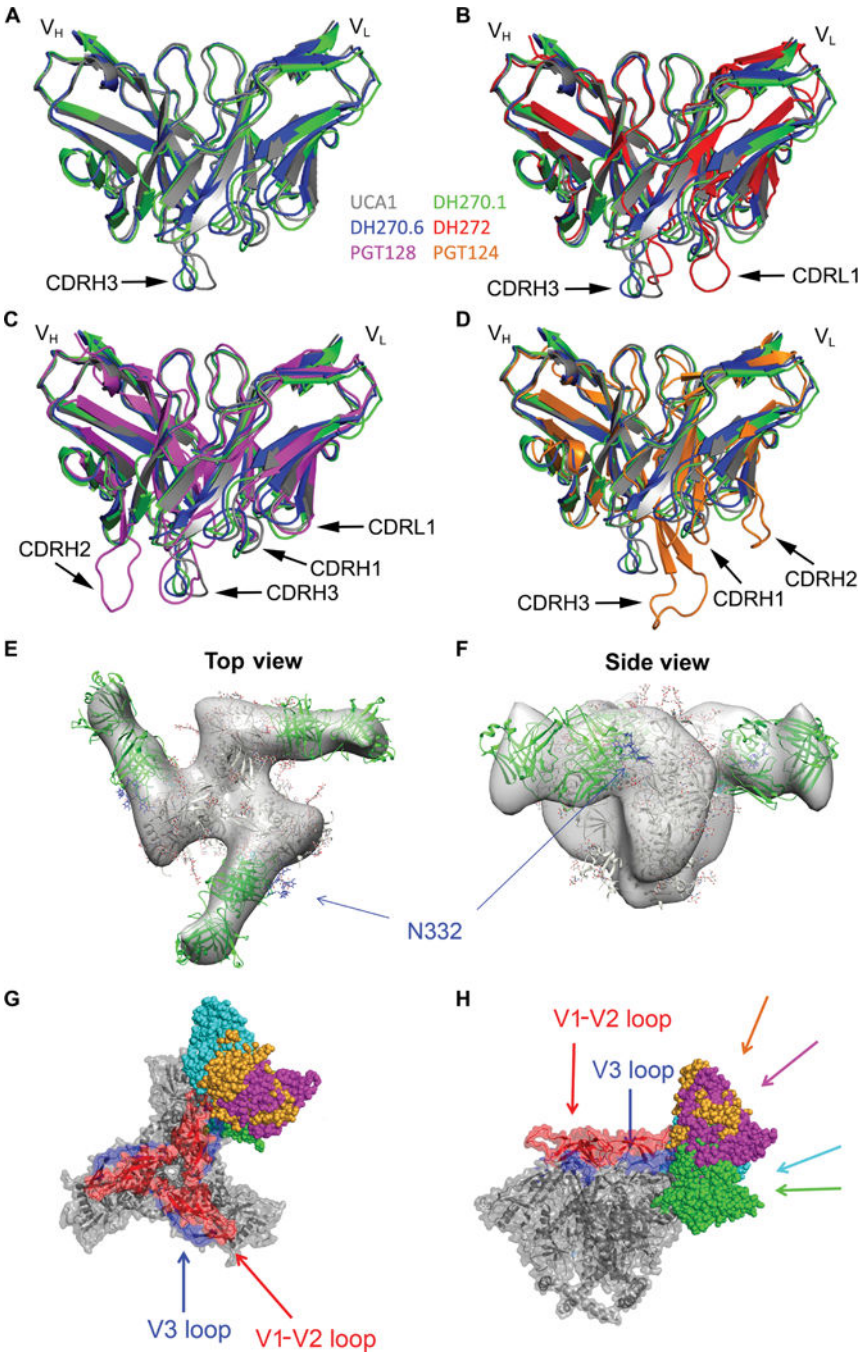

Fig. 5. Fab/scFv crystal structures and three-dimensional reconstruction of DH270.1 bound with the 92BR SOSIP.664 trimer

Superposition of backbone ribbon diagrams for the DH270 lineage members: UCA1 (gray), DH270.1 (green), and DH270.6(blue)alone(**A**), withtheDH272cooperating antibody (red) (**B**), with PGT128 (magenta) (**C**), and with PGT124 (orange) (**D**). Arrows indicate major differences in CDR regions. Top (**E**) and side (**F**) views of a fit of the DH270.1 Fab (green) and the BG505 SOSIP trimer (gray) onto a map obtained from negative-stain EM. Top (**G**) and side (**H**) views of the BG505 trimer [Protein Data Bank (PDB) ID: 5ACO] (28) (gray,

with V1-V2 and V3 loops highlighted in red and blue, respectively) bound to PGT124 (PDB ID: 4R2G) (27) (orange), PGT128 (PDB ID: 3TYG) (17) (magenta), PGT135 (PDB ID: 4JM2) (22) (cyan), and DH270.1 (green), superposed. The arrows indicate the direction of the principal axis of each of the bnAb Fabs; the color of each arrow matches that of the corresponding bnAb. See also fig. S18.

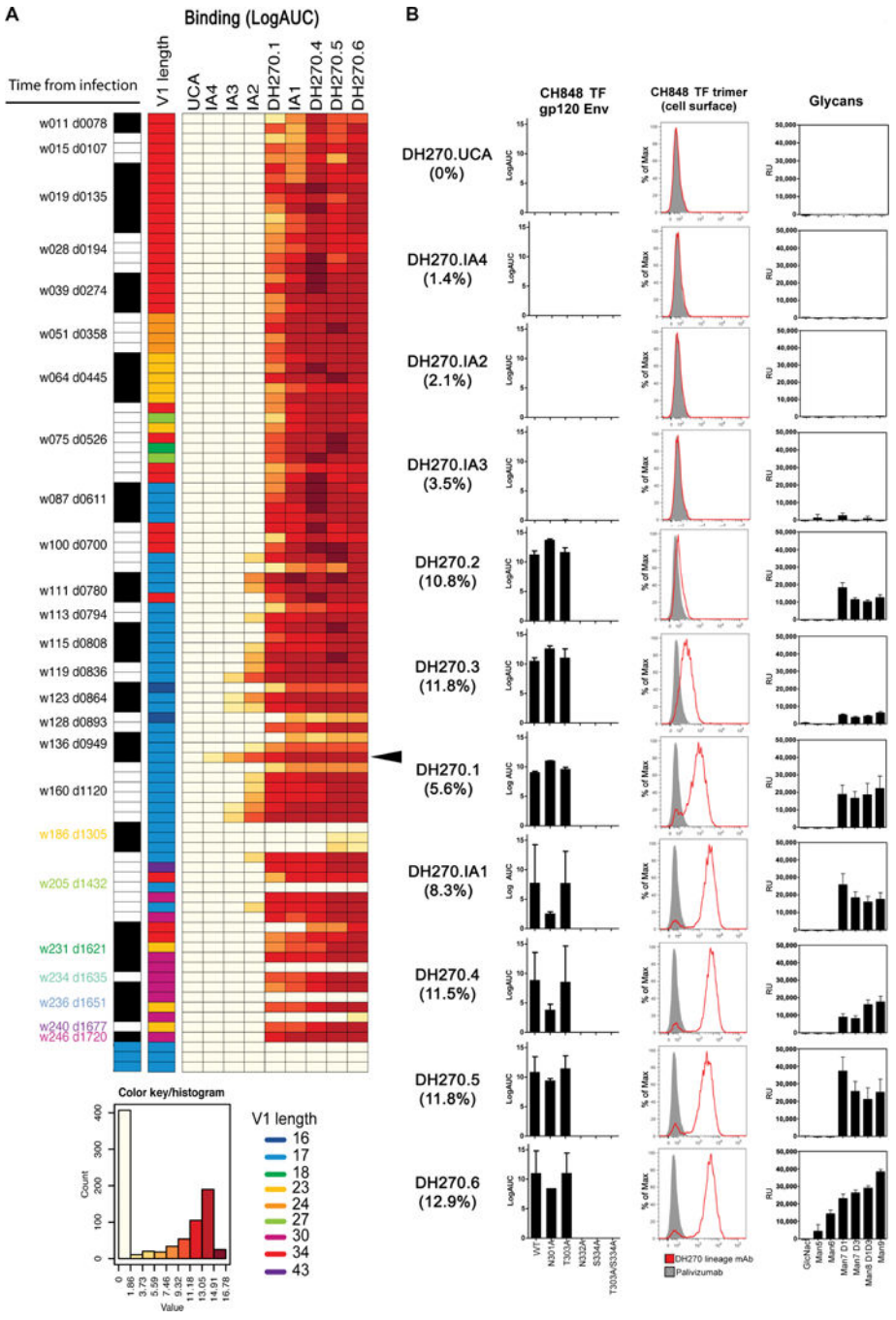

Fig. 6. DH270 lineage antibody binding to autologous CH848 Env components

(**A**) Binding of DH270 lineage antibodies (column) to 120 CH848 autologous gp120 Env glycoproteins (rows) grouped on the basis of time of isolation (w, week; d, day; black and white blocks). The last three rows show the neutralization profile of the three autologous viruses that lost the PNG at position N332 (blue blocks). V1 amino acid length of each virus is color-coded as indicated. Antibody binding is measured by enzyme-linked immunosorbent assay, expressed as log area under the curve (LogAUC), and color-coded on the basis of the categories shown in the histogram. The histogram shows the distribution of

the measured values in each category. The black arrow indicated Env 10.17. Viruses isolated at and after week 186, which is the time of first evidence of DH270 lineage presence, are highlighted in different colors according to week of isolation. (**B**) Left: Binding to CH848 TF mutants with disrupted N301 and/or N332 glycan sites. Results are expressed as LogAUC. V_H mutation frequency is shown in parentheses for each antibody (see also fig. S1A). Middle: Binding to CH848 Env trimer expressed on the cell surface of Chinese hamster ovary cells. Results are expressed as maximum percentage of binding and are representative of duplicate experiments. DH270 antibodies are in red. Palivizumab is the negative control (gray area). The curves indicate binding to the surface antigen on a scale of 0 to 100 (*y* axis); the highest peak between the test antibody and the negative control sets the value of 100. Right: Binding to free glycans measured on a microarray. Results are the average of background-subtracted triplicate measurements and are expressed in relative units (RU).